Hindawi
Wireless Communications and Mobile Computing
Volume 2018, Article ID 4704218, 13 pages
https://doi.org/10.1155/2018/4704218

Research Article

Improved Model for Estimation of Spatial Averaging Path Length

Pamela Njemčević,[1] Adriana Lipovac,[2] and Vlatko Lipovac[2]

[1]*Department of Telecommunications, Faculty of Electrical Engineering, University of Sarajevo, Sarajevo, Bosnia and Herzegovina*
[2]*Department of Electrical Engineering and Computing, University of Dubrovnik, Dubrovnik, Croatia*

Correspondence should be addressed to Pamela Njemčević; pamela.njemcevic@etf.unsa.ba

Received 16 March 2018; Revised 23 May 2018; Accepted 31 May 2018; Published 12 July 2018

Academic Editor: Enrico M. Vitucci

In mobile communication systems, the transmitted RF signal is subject to mutually independent deterministic path loss and stochastic multipath and shadow fading. As at each spatial location mostly the composite signal samples are measured, their components are distinguished by averaging out the multipath-caused signal level variations, while preserving just the ones due to shadowing. The prerequisite for this is the appropriateness of the local area averaging path length that enables obtaining the local mean (composed of mean path loss and shadow fading) and the multipath fading as difference between the composite signal sample and the local mean. However, the so far reported analytical approaches to estimation of the averaging path length are based on considering either the multipath or just the shadow fading, with applicability limited to only specific topologies and frequencies. Therefore, in this paper, the most widely used Lee analytical method is generalized and improved by considering multipath and shadowing concurrently, so providing the general closed-form elementary-function based estimation of the optimal averaging path length as a function of common multipath and shadow fading parameters characterizing particular propagation environment. The model enables recommendations for the optimal averaging length for all propagation conditions facing the mobile receiver.

1. Introduction

In a mobile communication system, the received RF signal, attenuated by deterministic path loss, varies in time and space stochastically [1]. Temporal variations are caused by moving objects near the stationary transmitter and receiver, while overall spatial variations are due to (mutually independent) shadowing and multipath propagation effects [2]. The shadowing-caused variations correspond to slow fading of the signal local mean that is noticeable only over large-scale receiver location changes (of the order of tens of wavelengths), implying constant local mean within these so-called local areas [3]. On the contrary, multipath fading occurs on a small-scale change of distance between transmitter and receiver (of the order of less than a wavelength), when constructive and destructive interference of multiple propagation paths (each exhibiting various amplitude, delay, and phase) cause fast signal variations even within local areas, so that the composite spatially variable received signal is finally affected by both fading types. Accordingly, with the real-life RF measurements, only the composite signal samples can be obtained. However, if the collected samples are to be used for particular channel modelling, it is necessary to distinguish slow and fast signal variations and process them separately in order to estimate their statistical distribution and relevant metrics, extensively used in wireless digital communication systems. So, e.g., while the multipath fading statistics is important for the transceiver design, as well as for the performance estimation (e.g., bit error rate (BER), outage probability), the shadow fading statistical description determines the automatic gain control parameters, as well as enabling optimization of the macroscopic propagation models for improved coverage on the area of interest and for evaluation of cell coverage area within already installed wireless systems.

Accordingly, it is necessary to correctly average the composite signal within each local area, i.e., to choose the optimal local averaging path length value, along which the

multipath-caused received signal level variations would be sufficiently integrated out, while preserving intact the ones caused exclusively by shadowing. This enables obtaining the shadow fading samples (proportional to the local mean) and so the multipath fading as a difference between the composite signal sample and the appropriate local mean at each spatial location.

With this regard, after some empirical methods with questionable accuracy, the first generally applicable analytical procedure for calculation of the appropriate averaging length [4, 5] evolved to the well-known Lee criteria, suggesting averaging the composite signal samples along the length between 20λ and 40λ. Although such recommendations have served for many years as a reference for spatial local averaging in outdoor environment with the Ultrahigh Frequency (UHF) band, these recommendations are not compliant with empirically obtained values for indoor environment at 900 MHz and 2 GHz (10λ) [6], or for urban cells with the lower Very High Frequency (VHF) band (6λ – 8λ) [7].

The lack of generality of Lee results is partially overcome in [1, 8–10], but the proposed models still cannot provide meaningful recommendations for urban and indoor environments with UHF band, as well as for mobile systems operating outside that band [11]. Namely, the models from [8–10] are focused on multipath averaging but neglect that the variations caused by shadowing should not be averaged along the (optimal) length, while the model in [1] is focused only on preserving the shadow fading constancy over the averaging length. Although these models can be used for estimation of the averaging length for limited combinations of multipath and shadow fading statistical parameters characterizing specific propagation conditions, it is shown [11] that still no recommendation can be derived for many other remaining parameter combinations. That is why the so far proposed analytical solutions lack generality with respect to propagation environment and frequency band [11].

Accordingly, in this paper, we extend the Lee method for estimating the appropriate averaging length by taking into account the variations caused by shadowing and multipath concurrently and developed the unified model which is applicable for all relevant propagation conditions facing the mobile receiver.

Since the herein proposed model is based on the Lee procedure, the latter is first introduced in detail in Section 2, and then the overview of other reported analytical models for estimating the averaging length is given. These models' drawbacks motivated derivation of the analytical expression as a function of common multipath and shadow fading parameters, to enable accurate local mean estimation and differentiation between shadow and multipath fading, without propagation and system restrictions, as it is presented in Section 3. With this regard, the optimal averaging path length values, obtained by applying the corresponding channel parameters' empirical values for particular propagation environments onto the analytical model, are presented in Section 4. Comparisons of recommendations for the averaging length values derived using the herein proposed model with widely used Lee's recommendations, as well as with the existing empirically based ones, are presented in Section 4.1, while conclusions are summarized in Section 5.

2. Models for Estimation of Spatial Averaging Path Length

2.1. Lee Model. Having passed the narrowband channel, the composite spatially variable received RF signal $r(x)$ can be expressed as [4]

$$r(x) = \mu(x)\, r_0(x). \tag{1}$$

where $\mu(x)$ and $r_0(x)$ denote its true mean value $\mu(x) = \langle r(x)\rangle$ and fast variations of the signal at spatial location x within a local area, respectively. Since only the composite signal values can be obtained by measurements, in order to perform accurate statistical modeling of slow and fast variations separately, it is a priori necessary to estimate the local means. Accordingly, in the Lee procedure, it is assumed that the estimated local mean $\hat{\mu}(x)$ can be obtained by integrating $r(x)$ along a certain path length $2L$ [4]

$$\hat{\mu}(x) = \frac{1}{2L}\int_{x-L}^{x+L} r(y)\, dy = \frac{1}{2L}\int_{x-L}^{x+L} r_0(y)\,\mu(y)\, dy \tag{2}$$

and that it approaches $\mu(x)$ when $2L$ becomes close to the optimal value $2L_a$.

Since the variance ${\sigma_{\hat{\mu}}}^2$ of the estimated mean $\hat{\mu}(x)$ around $\mu(x)$

$$\begin{aligned} {\sigma_{\hat{\mu}}}^2 &= \frac{1}{4L^2} \\ &\cdot \int_{x-L}^{x+L}\int_{x-L}^{x+L} \left[\langle r(y_1)\, r(y_2)\rangle - \langle r(y_1)\rangle \langle r(y_2)\rangle\right] dy_1 dy_2 \end{aligned} \tag{3}$$

can be expressed as a function of the autocorrelation function $R_r(x)$ of the received signal and its true mean value $\langle r(x)\rangle$ as well as of the length $2L$ [5]:

$${\sigma_{\hat{\mu}}}^2 = \frac{1}{L}\int_0^{2L}\left(1 - \frac{x}{2L}\right)\left[R_r(x) - \langle r(x)\rangle^2\right] dx \tag{4}$$

it is used in the Lee procedure as the local mean estimation error metric in terms of $2L$, based on the condition that 68% of $\hat{\mu}(x)$ values on $2L$ (where ${\sigma_{\hat{\mu}}}^2$ is assumed to be Gaussian random variable with the mean $\langle\hat{\mu}(x)\rangle = \mu(x)$ [5] and variance ${\sigma_{\hat{\mu}}}^2$) should be within the interval of two standard deviations $(\mu(x) - \sigma_{\hat{\mu}}, \mu(x) + \sigma_{\hat{\mu}})$ around the true mean $\mu(x)$ [5]. Accordingly, the optimal averaging length $2L_a$ is estimated by minimizing the local mean estimation error defined in logarithmic scale as $\sigma_{\hat{\mu}}spread(2L)$ [4, 5]:

$$\sigma_{\hat{\mu}}spread\,(2L) = 20\log\frac{1 + \sigma_{\hat{\mu}}/\langle r(x)\rangle}{1 - \sigma_{\hat{\mu}}/\langle r(x)\rangle}. \tag{5}$$

With Lee method, the proposed metric (5) was used for calculation of $2L_a$ under assumptions of constant $\mu(x)$ independent of $2L$ and Rayleigh-distributed $r_0(x)$ with its mean $\mu(x)$. Consequently, $\mu(x)$ is extracted in front of the

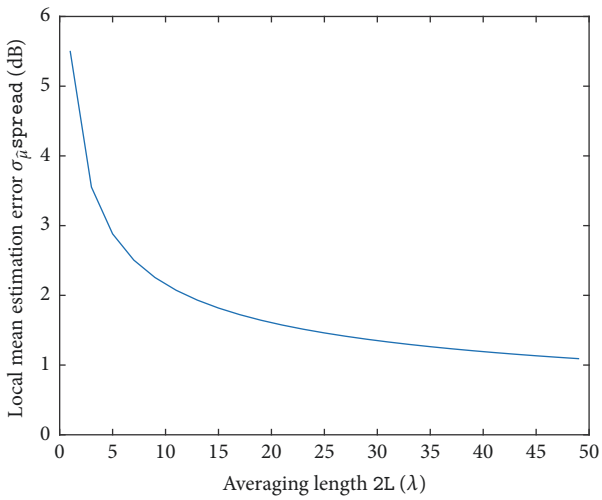

FIGURE 1: $\sigma_{\hat{\mu}}spread(2L)$ functions, obtained analytically by assuming Rayleigh multipath fading distribution and constant local mean for any $2L$ [4].

integral in (2), implying $r(x)$ to be also Rayleighian (with its easy-to-calculate autocorrelation function $R_r(x)$ and mean $\langle r(x)\rangle$ [5], which are substituted in (4)-(5) for calculation of $\sigma_{\hat{\mu}}spread(2L)$). This provided $\sigma_{\hat{\mu}}spread(2L)$ expressed as monotonically decreasing function of $2L$ (see Figure 1), which is used to derive recommendations for the appropriate averaging length value ($2L_a = 40\lambda$) by applying the analytically groundless assumption that the overall multipath variations can be neglected for the local mean estimation error up to 1 dB (i.e., $\sigma_{\hat{\mu}}spread(2L_a) = 1$ dB).

2.2. Other Models. However, in reality, the Rayleigh distribution presumption for multipath fading is mostly worst case, i.e., describing the most severe fast signal variations, particularly if line-of-sight between the transmitter and the receiver does not exist, implying applicability of previously developed recommendation only to some very specific propagation conditions.

Furthermore, considering channels with the multipath fading intensity less severe than in Rayleigh channels, by assuming the Rician [8, 9] or Nakagami-m multipath fading distribution [10] instead of the Rayleigh one, while still following the Lee approach (by assuming the local mean constancy on any $2L$ and maximal acceptable estimation error of 1 dB), this resulted with monotonically decreasing $\sigma_{\hat{\mu}}spread(2L)$ curves with recommendations for $2L_a$ dependent on the multipath fading severity (expressed by K or m parameter for Rician or Nakagamian distribution, respectively) of the observed propagation environment.

However, this still neglected that the assumption of constant $\mu(x)$ [4, 5, 8–10] is not applicable to just any $2L$ [1], but only if it does not exceed certain upper bound (from now on

$$\int_0^{2L} x \cdot J_0^2\left(\frac{2\pi x}{\lambda}\right) dx = 2L^2\left[J_0^2\left(\frac{2\pi \cdot 2L}{\lambda}\right) + J_1^2\left(\frac{2\pi \cdot 2L}{\lambda}\right)\right] \quad (6)$$

denoted as $2L_{sh}$), after which, in reality, the local mean $\mu(x)$ becomes function of $2L$ and the local mean estimation error (i.e., $\sigma_{\hat{\mu}}spread(2L)$) starts to increase again. Accordingly, before determination of $2L_a$, it is first necessary to calculate $2L_{sh}$ for the target environment with its shadow fading severity reflected by the lognormal standard deviation (in logarithmic scale) σ_{dB} and decorrelation distance D. This task was accomplished in the previous work [1], where $2L_{sh}$ was identified as the maximal averaging length for which the local mean correlation coefficient $\rho(2L)$:

$$\rho(x) = \frac{\left(R_{\mu(x)} - \langle \mu(x)\rangle^2\right)}{\sigma_{\mu(x)}{}^2} \quad (7)$$

(with $\langle\mu(x)\rangle$, $\sigma_{\mu(x)}{}^2$, and $R_{\mu(x)}$ representing the mean, the variance, and the autocorrelation function of the true mean $\mu(x)$, respectively) is larger than or equal to 0.8 (in linear domain), indicating that, for any $2L \le 2L_{sh}$, the local mean can be considered highly autocorrelated or approximately constant [1].

Accordingly, the so far available analytical expressions applies for estimation of the averaging length lower bound $2L_{mp}$ that enables good enough averaging out of multipath fading [4, 5, 8–10], as well as for estimation of the averaging length upper bound ($2L_{sh}$) [1] that enables $\mu(x)$ to remain constant on $2L$. If, for the adopted shadow and multipath fading parameters describing particular propagation conditions, $2L_{mp} \le 2L_{sh}$ (as it is the case for $m = 2$, $\sigma_{dB} = 7$ dB, and $D = 200$ m at $f = 1$ GHz, which characterize suburban outdoor environment with UHF band; see Section 3), the optimal averaging length $2L_a$ can be considered to be in between $2L_{mp}$ and $2L_{sh}$ (since $2L_{mp} \approx 30\lambda$ [10] and $2L_{sh} \approx 100\lambda$ [1]).

However, if $2L_{mp} > 2L_{sh}$ is obtained (which is the case for the following combination of parameters: $m = 1$, $\sigma_{dB} = 7$ dB, and $D = 40$ m at $f = 1$ GHz, characterizing outdoor urban cells with UHF, where $2L_{mp} = 45\lambda$ [10] and $2L_{sh} = 20\lambda$ [1]), simultaneously fulfilling both criteria: $\sigma_{\hat{\mu}}spread(2L_a) \le 1$ dB (obtained by assuming just multipath variations) and $\rho(2L) \ge 0.8$ (obtained by assuming just shadowing variations) is not possible and so is to proceed with estimation of $2L_a$ that would have been appropriate for these propagation environments [11]. Moreover, even in the case when $2L_{mp} \le 2L_{sh}$, still both bounds arise from the analytically groundless, i.e., subjective, criteria that $\sigma_{\hat{\mu}}spread(2L_{mp}) \approx 1$ dB [4]) and $\rho(2L_{sh}) \approx 0.8$ [1], with no analytical proof that multipath and shadow fading are really constant enough at these bounds.

In addition, though so far no analytical hint exists for estimating $2L_a$ regardless of propagation specifics and beyond subjectively chosen criteria, still some recent empirical $2L_a$ estimations were proved to be accurate, unambiguous, and objective by processing measured composite signal samples, i.e., by treating shadow and multipath fading on $2L$ not separately but concurrently [12]. This approach resulted with the U-shaped curves of the $\sigma_{\hat{\mu}}spread(2L)$ function (reflecting both multipath and shadowing residual variations along $2L$) [7, 12] instead of the monotonically decreasing curves for residual multipath-only variations, thus identifying $2L_a$ as the

curve minimum, rather than using the subjective 1 dB Lee criterion.

Still, this empirical approach requires acquisition of many composite signal samples, which is time-consuming and implies lower significance of empirical methods for $2L_a$ estimation and motivates development of a general analytical algorithm. However, the idea of concurrent treatment of shadow and multipath fading is definitely what must be adopted from the referenced empirical methods, since thus obtained U-shaped spread curves exhibit $2L_a$ as a minimum for all possible combinations of m, σ_{dB}, and D, thus avoiding potentiality intuitive selection of $2L_a$ in the propagation conditions with $2L_{mp} > 2L_{sh}$ ($2L_a$ should be chosen so as to comply with $2L_{mp} \leq 2L_a \leq 2L_{sh}$).

3. Extension of the Lee Method for Estimating Optimal Averaging Path Length

In contrast to the Lee analytical approach, based on (2)–(5), in which the local mean $\mu(x)$ was assumed constant regardless of $2L$ value, thus effectively enabling processing of the composite signal $r(x)$ distribution as if only multipath fading was present and results with monotonically decreasing $\sigma_{\tilde{\mu}}spread(2L)$ function, no such limiting assumption is made here. Instead, both the residual slow and fast variations of the entire composite signal samples on $2L$ are taken into account for estimating $\sigma_{\tilde{\mu}}spread(2L)$.

Thus, in order to calculate $\sigma_{\tilde{\mu}}spread(2L)$ by (5), we first assume the distribution of $r(x)$, which we consider to be the most convenient for describing propagation in mobile systems and then derive the appropriate first- and second-order statistics, i.e., its mean value $\langle r(x)\rangle$ and autocorrelation function $R_r(x)$. Thereby, similarly as Lee [4, 5] and his successors [8, 9], we also focus our analysis on narrowband channels, as, e.g., in 2G, channel bandwidth is 200 kHz in the 1 GHz band, while in 4G, the OFDM subchannels are 15 kHz wide etc.

So, following the above scenario, in this paper, we consider the Generalized K distribution (mixture of Nakagami-m and Gamma distributions describing multipath and shadow fading statistics, respectively) as most convenient for the target systems [13]:

$$f_{r(x)} = \frac{4}{\Gamma(m)\Gamma(k)}\left(\frac{m}{\Omega}\right)^{(k+m)/2} \cdot r(x)^{m+k-1} K_{k-m}\left(2\sqrt{\frac{m}{\Omega}}r(x)\right) \quad m \geq \frac{1}{2},\ k > 0,\ \Omega > 0 \tag{8}$$

where $\Gamma(\cdot)$ denotes the Gamma function and $K_{k-m}(\cdot)$ the modified Bessel function of the second kind and order $(k - m)$. The Nakagami parameter m inversely reflects severity of multipath fading [14], while scale parameter Ω is the mean of local average power envelope [13]. The shape parameter k inversely reflects Gamma shadow fading severity [13] and is related to the lognormal shadow fading standard deviation σ_{dB} as follows [13, 14]:

$$k = \frac{1}{e^{(0.115\sigma_{dB}{}^2)} - 1} \tag{9}$$

where σ_{dB} is expressed in dB units, reflecting the common practice with regard to normal probability density function (pdf) coming out of measurement campaigns.

Although any composite signal distribution could be adopted into (3)–(5), the Nakagami-Gamma distribution of $r(x)$ is chosen here since the Nakagami-m distribution is flexible enough to describe multipath fading conditions of variable severity, in a mathematically convenient way [15] and consistently with empirical data [14, 16–18], while the Gamma distribution is much superior to other ones (including the usually used lognormal distribution) for shadow fading analytical modeling [15], still remaining consistent with empirical data regarding terrestrial and satellite channels in variety of frequency bands [19].

Having adopted these assumptions, $\langle r(x)\rangle$ is calculated using the integral transformation form, as follows [20]:

$$\langle r(x)\rangle = \sqrt{\left(\frac{\Omega}{m}\right)}\frac{\Gamma(k+1/2)\Gamma(m+1/2)}{\Gamma(m)\Gamma(k)} \tag{10}$$

while $R_r(x)$ is derived based on the bivariate Generalized K pdf [21] and the calculated product of its moments of the order $n_1 + n_2$ [21, eq.6] (since the autocorrelation function of the Generalized K-distributed process can be calculated as the moment of the product of joint Generalized K variables of the first order, i.e., when $n_1 = n_2 = 1$), as

$$R_r(x) = \langle r(x)\rangle^2 \cdot {}_2F_1\left(-\frac{1}{2},-\frac{1}{2};m;\rho_N(x)\right){}_2F_1\left(-\frac{1}{2},-\frac{1}{2};k;1-\rho_G(x)\right) \tag{11}$$

where the first two parameters −0.5 within both hypergeometric functions are obtained by substitution of $n_1 = n_2 = 1$ values in n_1+n_2 product moment expression [21, eq. 6]. $\rho_N(x)$ and $\rho_G(x)$ denote the power correlation coefficient between two squared Nakagami envelope samples and the correlation coefficient between two samples of Gamma local mean power [21], respectively. Here ${}_2F_1(.)$ represents the Gaussian hypergeometric functions whose utmost right parameter is adopted as monotonically decreasing function of distance x when it reflects multipath fading, and as monotonically increasing function of x when it reflects variations caused by shadowing, since local mean estimation error due to residual multipath variations along the chosen averaging length decreases with distance, while the error caused by inappropriately averaged shadow fading increases when averaging length exceeds the local area.

Furthermore when the squared Nakagami-m envelope is expressed as a sum of sinusoidal, independent, and identically distributed squared Rayleigh envelopes [22], its correlation coefficient for narrowband channels can be calculated as [10]

$$\rho_N(x) = J_0^2\left(\frac{2\pi x}{\lambda}\right) \tag{12}$$

where $J_0(.)$ is the first-kind Bessel function of order zero and the simplest isotropic multipath fading scenario with uniformly distributed angles of arrivals (AoA) is assumed (although more general expression, based on nonisotropic fading scenario with nonuniform distribution of AoA, can be used instead) [10].

On the other hand, the Gamma local mean correlation coefficient $\rho_G(x)$ is approximated by lognormal local mean correlation coefficient $\rho_L(x)$ [1] (obtained following the Gudmundson shadowing correlation models [23]), due to excellent match between the lognormal and Gamma pdfs [13, 14]:

$$\rho_G(x) \approx \frac{e^{((0.115\sigma_{\mathrm{dB}})^2 e^{-|x|/D})} - 1}{e^{(0.115\sigma_{\mathrm{dB}})^2} - 1} \tag{13}$$

where D denotes the shadowing decorrelation distance (expressed in meters) of the propagation environment, at which the signal autocorrelation equals 1/e of its maximum value [23].

Accordingly, by substituting (9), (12), and (13) in (11), (9), (10), and (11) in (4) and finally (4) and (10) in (5), the relative spread $\sigma_{\widehat{\mu}}spread(2L)$ of the estimated mean $\widehat{\mu}$(x) around the true mean $\mu(x)$ of the Generalized-K-distributed composite signal for a particular propagation environment of interest, is finally expressed as a function of $2L$:

$$\sigma_{\widehat{\mu}}spread(2L; m, \sigma_{dB}, D) = 20 \cdot \log \frac{1 + \sqrt{(1/L)\int_0^{2L}(1 - x/2L)\left\{{}_2F_1\left[-1/2, -1/2; m; J_0^2(2\pi x/\lambda)\right] {}_2F_1\left[-1/2, -1/2; 1/\left(e^{(0.115\sigma_{\mathrm{dB}})^2} - 1\right); 1 - \left(e^{((0.115\sigma_{\mathrm{dB}})^2 e^{-|x|/D})} - 1\right)/\left(e^{(0.115\sigma_{\mathrm{dB}})^2} - 1\right)\right] - 1\right\} dx}}{1 - \sqrt{(1/L)\int_0^{2L}(1 - x/2L)\left\{{}_2F_1\left[-1/2, -1/2; m; J_0^2(2\pi x/\lambda)\right] {}_2F_1\left[-1/2, -1/2; 1/\left(e^{(0.115\sigma_{\mathrm{dB}})^2} - 1\right); 1 - \left(e^{((0.115\sigma_{\mathrm{dB}})^2 e^{-|x|/D})} - 1\right)/\left(e^{(0.115\sigma_{\mathrm{dB}})^2} - 1\right)\right] - 1\right\} dx}} \tag{14}$$

In Figure 2, typical $\sigma_{\widehat{\mu}}spread(2L)$ plots according to (14) are presented for 4 ad hoc chosen exemplar combinations of m, σ_{dB}, and D values. The curves are obviously U-shaped, just as their empirically obtained counterparts [7, 12], which has already been mentioned in Section 2 to enable straightforward identification of the optimal averaging path length $2L = 2L_a$ as the minimum.

Comparing the observations from Figure 2 with the results obtained by using other analytical models, it can be seen that, by reducing the multipath fading severity m, $2L_a$ shifts left taking smaller values, while $\sigma_{\widehat{\mu}}spread(2L)$ drops significantly, which is consistent with analytical $2L_{mp}$ estimations [8–10]. Moreover, by increasing σ_{dB} or decreasing D, $\sigma_{\widehat{\mu}}spread(2L)$ increases, while $2L_a$ shifts left toward smaller values, which is consistent with analytical $2L_{sh}$ estimation [1].

However, the main task of the proposed approach is to provide recommendations for the optimal averaging length $2L_a$ enabling minimal values of $\sigma_{\widehat{\mu}}spread(2L)$ function for specific environments described by parameters m, σ_{dB}, and D. With this regard, differentiating very complex expression (14) with respect to $2L$ is anything but simple and can only be accomplished through a number of successive approximations, based on prior assessment and comparison of particular m, σ_{dB}, and D values.

Accordingly, for the environments with $m \geq 1$ (describing Rayleigh and less severe multipath fading channels) and $0 < 2L \ll D$, the elementary-function-based implicit expression for the optimal averaging path length $2L = 2L_a$ is derived in the Appendix as (A.37) and accordingly rewritten here as follows:

$$\frac{(0.115\sigma_{\mathrm{dB}})^2 e^{(0.115\sigma_{\mathrm{dB}})^2}}{3D/\lambda}\left(\frac{2L_a}{\lambda}\right)^2 - \frac{1}{m\pi^2}\left[\ln\left(2\pi\frac{2L_a}{\lambda} + 0.67\right)\right] = 0 \tag{15}$$

which is wavelength-independent (if D and $2L$ are expressed as multiples of λ) and obviously much more computationally efficient than finding the minimum from an integral equation such as (14).

Thus, by means of (15), $2L_a$ can be evaluated for any combination of the relevant parameters m, σ_{dB} and D, which was not possible with other analytical models.

4. Recommendations for Optimal Averaging Path Length in Various Propagation Conditions

The derived expression (15) is to be used now to derive recommendations for optimal averaging path length in various propagation environments, represented in (15) by the corresponding values of multipath and shadowing parameters obtained empirically. Thereby, in order to avoid any subjectivity and partiality which might arise from our own measurements, the values of $m, \sigma_{\mathrm{dB}}, D$ are collected from the relevant literature. However, empirical determination of any particular values of parameters $m, \sigma_{\mathrm{dB}}, D$, presumes prior separation of shadow and multipath fading, for what assuming a certain value of the averaging length is a prerequisite. Accordingly, in order to avoid adopting potentially inaccurate specific values of $m, \sigma_{\mathrm{dB}}, D$ in relevant papers, we determine boundaries of each parameter in various propagation environments and frequency bans, instead.

So, considering the shadow and multipath fading facing the mobile receiver in urban cells operating in 0.9 – 2.4 GHz band (e.g., [23–26]), the multipath fading was found to be very severe – with quite pronounced envelope variations usually described by Rayleigh distribution (or Nakagami with $m = 1$). The shadowing standard deviations from the mean path losses are mostly much bigger than in other environments and typically take values between 7 and 9 dB,

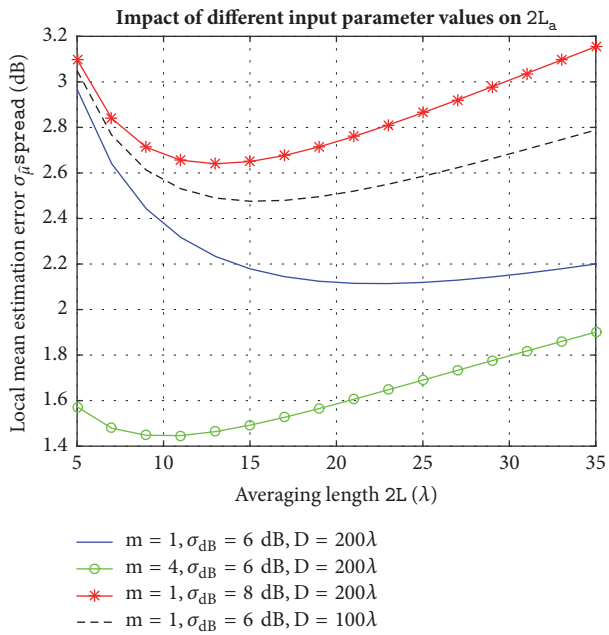

Figure 2: $\sigma_{\hat{\mu}}spread(2L)$ functions for different sets of input parameters m, σ_{dB}, and D.

while the decorrelation distance can be considered to be between 30 and 50 m.

The multipath fading in suburban cells with UHF band is less severe than in urban ones, and can be modelled by Nakagami distribution with m between 2 and 4. Similarly, the suburban shadowing standard deviations are mostly smaller than in urban environments, and can be described with σ_{dB} between 5 and 7 dB, while the decorrelation distance due to topological characteristics, can be taken to be between 200 and 300 m (e.g., [23, 27, 28]).

In rural cells, the shadow fading shows similar characteristics as in suburban cells, with slightly bigger decorrelation distance $D > 300$ m, while the multipath fading usually exhibits smaller dips and slower changes, and can be described by Nakagami-m distribution, with m between 4 and 8 (e.g., [27, 29]).

Finally, by analysing the shadow and multipath fading in indoor cells, it can be seen that the multipath has similar characteristics as in suburban cells (m between 2 and 4), while the shadowing standard deviation is the smallest among all of the environments, and the decorrelation distance due to topology is usually between 3 and 5 m (e.g., [30, 31]).

The adopted boundaries of the multipath and shadow fading parameters, for various environments with UHF band, are listed in Table 1.

Moreover, as beside the UHF band, the VHF band and the lower Super High Frequency (SHF) band are also used for mobile communications (where similar 1st and 2nd order signal statistics applies as in UHF), boundaries of multipath and shadow fading parameters have to be adopted also for frequencies slightly beyond the UHF band.

From a number of papers such as [32], it has come out that the decorrelation distance is practically independent on frequency, while the shadowing standard deviation changes for about 1 to 2 dB between different frequency bands (e.g., VHF and UHF). Accordingly, in urban cells with mobile systems operating below the UHF band, the shadowing standard deviation should be adopted between 5 and 7 dB, and between 8 and 10 dB for the lower SHF band [33, 34], while the multipath shows similar behaviour regardless the operating frequency band (Table 2).

Accordingly, substitution of the adopted values for the multipath and shadow fading boundaries from Tables 1 and 2 into (15) provides the recommendations for the optimal averaging length values listed in Table 3.

Since the boundaries rather than exact values of recommended $2L_a$ values are given in Table 3, it is important to investigate the impact of the adopted $2L_a$ values on the local mean estimation error. For this purpose, the proposed values of shadow and multipath fading parameters are substituted into (14), which is graphed in Figure 3 for UHF band.

From Figure 3 it can be seen that, in urban UHF cells, the local mean estimation error remains within 5% of its minimal value if $2L_a$ is chosen anywhere within the proposed boundaries from Table 3. However, if local averaging is performed according to the Lee recommendation of 40λ, $\sigma_{\hat{\mu}}spread(2L)$ becomes 30% worse than it could be obtained by adopting the optimal averaging length, thus indicating the importance of appropriate selection of the spatial averaging length in these environments.

Similarly, with indoor cells, averaging along the path length within $5\lambda - 15\lambda$ results with about 5% deviation of the

Table 1: Adopted boundaries of multipath and shadowing parameters for various environments with UHF band.

Cell type	m	σ_{dB} (dB)	D (m)
Urban	1	7 – 9	30 – 50
Suburban	2 – 4	5 – 7	200 – 300
Rural	4 – 8	5 – 7	> 300
Indoor	2 – 4	< 5	3 – 5

Table 2: Adopted boundaries of multipath and shadowing parameters for various frequency bands in urban cells.

Frequency band (urban cells)	m	σ_{dB} (dB)	D (m)
Below the UHF band	1	5 – 7	30 – 50
UHF	1	7 – 9	30 – 50
Lower SHF	1	8 – 10	30 – 50

Table 3: Recommendations for optimal averaging length in various propagation environments and frequency bands.

Frequency band	Cell type	$2L_a$
UHF	Urban	$10\lambda - 20\lambda$
UHF	Suburban	$20\lambda - 50\lambda$
UHF	Rural	$20\lambda - 50\lambda$
UHF	Indoor	$5\lambda - 10\lambda$
Below the UHF band	Urban	$<10\lambda$ or $\sim 5\lambda$
Lower SHF	Urban	$>50\lambda$ or $\sim 80\lambda$

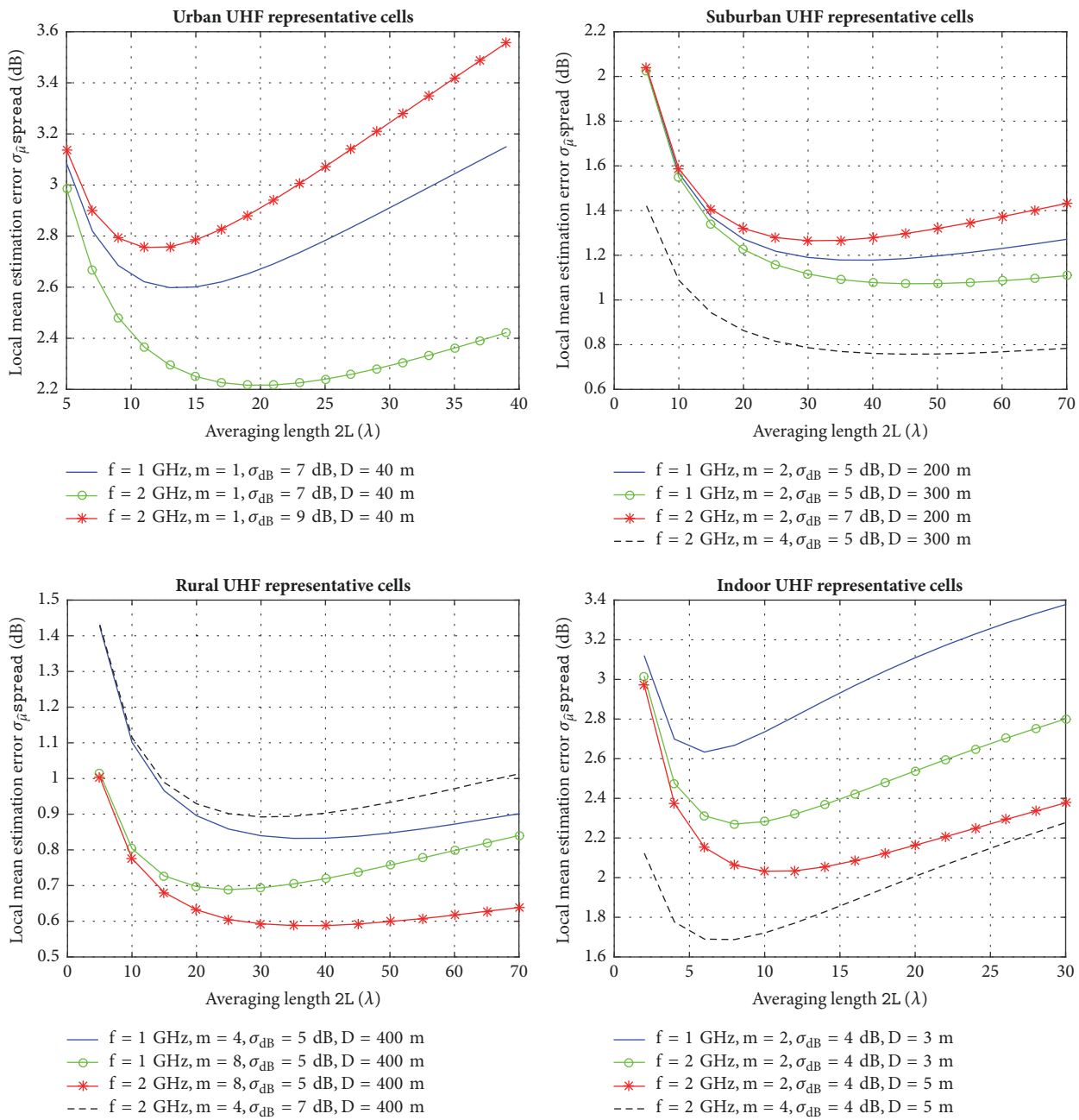

FIGURE 3: $\sigma_{\hat{\mu}}spread(2L)$ function for various input parameters representing typical topologies with UHF band.

estimation errors with respect to their minimal values, while, for larger lengths, the errors become unacceptable (e.g., equal to 50% for $2L = 40\lambda$).

However, in suburban and rural UHF cells, due to small estimation errors obtained within large $2L$ range, local averaging can be performed along any path length between 20λ and 70λ with acceptable sample mean error.

Analogously, in urban cells with mobile systems operating below the UHF band, local averaging should be performed along any path length between 1λ and 10λ, due to small relative difference between the so obtained and the minimal local mean estimation error for a given set of parameters. If local averaging is performed along 40λ, the local means include not only the multipath, but the averaged shadowing-caused variations, too, leading to huge local mean estimation error (with $\sigma_{\hat{\mu}}spread$ equal to 50% with respect to its minimal value).

Moreover, with high frequency mobile systems, local averaging should be done along the lengths longer than 50λ, since smaller lengths would lead to huge local mean estimation error due to insufficiently smoothed multipath fading along that length.

4.1. Comparison with the Existing Recommendations. Finally, the recommendations for adoption of $2L_a$ coming out of the herein proposed model are compared with the widely

Table 4: Comparison of derived recommendations with existing analytical and empirical results.

Frequency band /cell type	Modeled $2L_a$	Other analytical or empirical $2L_a$
UHF/urban	$10\lambda - 20\lambda$	
UHF/suburban	$20\lambda - 50\lambda$	Lee analytical recommendations [4, 5]: $20\lambda - 40\lambda$
UHF/rural	$20\lambda - 50\lambda$	
UHF/indoor	$5\lambda - 10\lambda$	Empirical recommendations [6]: $8\lambda - 10\lambda$
Below the UHF band/urban	$\lambda - 10\lambda$	Empirical recommendations [7]: $6\lambda - 8\lambda$
Lower SHF/urban	$50\lambda - 100\lambda$	-

used Lee recommendations and the existing empirical ones.

From Table 4, it can be seen that the recommendations based on (14) and (15): $10\lambda - 50\lambda$ for UHF outdoor, considerably overlap with Lee's and other widely used recommendations for $2L_a$: $20\lambda - 40\lambda$, for UHF outdoor in such environments. However, the former are more precisely segmented regarding the environment type, thus significantly improving the accuracy of local mean estimation, expressed by the widely used Lee metric $\sigma_{\hat{\mu}} spread(2L)$. This explains why Lee recommendations, though based on incomplete analytical model, provide acceptable recommendations for UHF band in outdoor cells.

Moreover, the model, articulated by (14)/(15) analytically derives the recommendations for UHF indoor, as well as for the mobile systems operating slightly beyond the UHF band. Recommendations for $2L_a$, as well as the assumptions about shadowing and multipath parameters boundaries (given in Tables 1 and 2), can be verified by the corresponding empirically backed recommendations [6, 7] for indoor cells at 0.9 GHz and 2 GHz ($8\lambda - 10\lambda$) [6] and for urban cells operating below the UHF band ($6\lambda - 8\lambda$) [7] (see Table 4 for comparison).

Additionally, the idea behind the model treating composite multipath and shadow fading concurrently could be further extended to any frequency band and wireless system, taking into consideration the appropriate 1st and 2nd order multipath and shadow fading statistics (instead of expressions (7) – (13)).

It is worth pointing out that improved $2L_a$ estimation accuracy enhances the local mean estimation accuracy. Thereby, more accurate local mean, used within handoff and adaptive modulation/coding algorithms, improves mobile system capacity, as well as improving coverage.

5. Conclusion

Real-life RF measurements provide composite signal samples, but often distinct multipath and shadow fading statistics and related metrics are needed in practice. The former is important for transceiver design, as well as for estimation of the performance, *BER*, outage probability etc., while the latter determines the automatic gain control parameters, as well as enableing optimization of the macroscopic propagation models. Thereby, for distinguishing of variations caused by shadowing and multipath, it is necessary to average the composite samples along the appropriate averaging length. With this regard, the so far proposed analytical solutions lack generality with respect to propagation environment and frequency band, providing recommendations only for specific combinations of multipath and shadow fading parameters. So, there is a need for a more general averaging length estimation approach, based on realistic and integral assumptions on both shadow and multipath fading and thus being applicable for all relevant propagation conditions.

By using the derived expression for the optimal averaging length, the recommendations for the appropriate values of averaging length in various propagation environments and frequency bands are derived: the optimal averaging path length values, obtained by applying the according parameters' empirical values boundaries for particular propagation environments onto the analytical model, pointed out that the optimal averaging length range in UHF band for rural and suburban cells is between 20λ and 50λ; for urban cells, it is between 10λ and 20λ, while, indoors, the values between 5λ and 10λ are shown to be most appropriate; in urban cells with mobile systems operating slightly above the UHF band, the local averaging should be done along the length of about 80λ, while below the UHF band, it is less than 10λ.

It is also shown that, compared to other state-of-the-art analytically backed recommendations, the herein proposed ones provide much smaller local mean estimation error in various propagation conditions and so they potentially improve performance of handoff and adaptive modulation/coding algorithms within real-life mobile systems.

Besides, the herein proposed recommendations, regarding averaging length values, are verified to be consistent with other analytically backed ones (but just in specific propagation environments where their related models apply), as well as with the corresponding empirically evaluated values in various frequency bands and propagation environments.

Appendix

Closed-Form Estimation of the Optimal Averaging Path Length

Finally, let us precisely locate the optimal averaging path length $2L = 2L_a$, by applying the standard condition for minimum to $\sigma_{\hat{\mu}} spread(2L)$ function (14):

$$\frac{d\left[\sigma_{\hat{\mu}} spread\,(2L; m, \sigma, D)\right]}{d\,(2L)} = 0. \tag{A.1}$$

As logarithmic function is monotonic, (A.1) can be simplified as

$$\frac{d\left[\left(1+\sqrt{(1/L)\,I(L)}\right)/\left(1-\sqrt{(1/L)\,I(L)}\right)\right]}{d(2L)}=0 \tag{A.2}$$

where

$$I(L)=\int_0^{2L}\left(1-\frac{x}{2L}\right)\cdot(\Pi(x)-1)\,dx \tag{A.3}$$

and Π(x) is the product of the two Gaussian hypergeometric functions:

$$\begin{aligned}&\Pi(x)\\&=\ {}_2F_1\left[-\frac{1}{2},-\frac{1}{2};m;J_0^2\left(\frac{2\pi x}{\lambda}\right)\right]\\&\quad\cdot\ {}_2F_1\left\{-\frac{1}{2},-\frac{1}{2};k;1-k\cdot\left[\left(1+\frac{1}{k}\right)^{e^{-|x|/D}}-1\right]\right\}.\end{aligned} \tag{A.4}$$

Moreover, we even do not have to calculate derivation in (A.1) and (A.2), as spread (14) will be minimal when the numerator is minimal and the denominator is maximal, which in turn occurs when $I(L)/L$ is minimal, so condition (A.1)/(A.2) further simplifies to

$$\begin{aligned}\frac{d\left[(1/L)\,I(L)\right]}{d2L}&=0\Longrightarrow\\ \frac{dI(L)}{d2L}&=\frac{I(L)}{2L}.\end{aligned} \tag{A.5}$$

Now let us develop (A.3) as follows:

$$I(L)=\int_0^{2L}\Pi(x)\,dx-\frac{1}{2L}\int_0^{2L}x\cdot\Pi(x)\,dx-L. \tag{A.6}$$

Bearing in mind the expansion of the Gaussian hypergeometric function in series [35]:

$$\begin{aligned}{}_2F_1[\alpha,\beta,\gamma;x]&=1+\frac{\alpha\beta}{1!\gamma}x+\frac{\alpha(\alpha+1)\beta(\beta+1)}{2!\gamma(\gamma+1)}x^2\\&\quad+\dots\end{aligned} \tag{A.7}$$

and, considering the actual m values as: $m\geq 1$, we notice that

$$\begin{aligned}\frac{J_0^2((2\pi\cdot 2L)/\lambda)}{4m}&>>\frac{J_0^4((2\pi\cdot 2L)/\lambda)}{32m\cdot(m+1)};\\ \left|J_0\left(\frac{2\pi\cdot 2L}{\lambda}\right)\right|&<1.\end{aligned} \tag{A.8}$$

So therefore we can justifiably approximate

$${}_2F_1\left[-\frac{1}{2},-\frac{1}{2};m;J_0^2\left(\frac{2\pi x}{\lambda}\right)\right]\approx 1+\frac{J_0^2(2\pi x/\lambda)}{4m}. \tag{A.9}$$

Furthermore, since in outdoor environment it is $2L\ll D$, and apparently

$$\frac{1}{8}\cdot\left[1-\left(\frac{k}{k+1}\right)^{2L/D}\right]<<1. \tag{A.10}$$

It implies (especially but not necessarily when $\gg 1$) that

$$\begin{aligned}&\frac{1-k\cdot\left[(1+1/k)^{e^{-|2L|/D}}-1\right]}{4k}\\&\quad>>\frac{\left\{1-k\cdot\left[(1+1/k)^{e^{-|2L|/D}}-1\right]\right\}^2}{32k\cdot(k+1)}.\end{aligned} \tag{A.11}$$

So that we can justifiably approximate

$$\begin{aligned}&{}_2F_1\left\{-\frac{1}{2},-\frac{1}{2};k;1-k\cdot\left[\left(1+\frac{1}{k}\right)^{e^{-|x|/D}}-1\right]\right\}\\&\quad\approx 1+\frac{1-k\cdot\left[(1+1/k)^{e^{-|x|/D}}-1\right]}{4k}.\end{aligned} \tag{A.12}$$

Consequently, product (A.4) of the two Gaussian hypergeometric functions becomes

$$\begin{aligned}\Pi(x)&=\left[1+\frac{J_0^2(2\pi x/\lambda)}{4m}\right]\\&\quad\cdot\left\{1+\frac{1-k\cdot\left[(1+1/k)^{e^{-x/D}}-1\right]}{4k}\right\}\end{aligned} \tag{A.13}$$

Again, since for outdoor it is $x\ll D$, it implies

$$\begin{aligned}\left(1+\frac{1}{k}\right)^{e^{-x/D}}&\approx\left(1+\frac{1}{k}\right)^{\cdot 1-x/D}\\&=\left(1+\frac{1}{k}\right)\cdot e^{-\ln(1+1/k)\cdot x/D}.\end{aligned} \tag{A.14}$$

As it is also $\ln(1+1/k)<1$, then (A.14) simplifies to

$$\left(1+\frac{1}{k}\right)^{e^{-x/D}}\approx\left(1+\frac{1}{k}\right)\cdot\left[1-\ln\left(1+\frac{1}{k}\right)\cdot\frac{x}{D}\right] \tag{A.15}$$

so that (A.13) can be rewritten as

$$\begin{aligned}\Pi(x)&=\left[1+\frac{J_0^2(2\pi x/\lambda)}{4m}\right]\\&\quad\cdot\left[1+\frac{\ln(1+1/k)^{1+1/k}}{4D}\cdot x\right]\end{aligned} \tag{A.16}$$

and so (A.6) as

$$\begin{aligned} I(L) = {} & 2L + \frac{1}{4m}\int_0^{2L} J_0^2\left(\frac{2\pi x}{\lambda}\right)dx \\ & + \frac{\ln(1+1/k)^{1+1/k}}{4D}\cdot\frac{4L^2}{2} + \frac{1}{4m} \\ & \cdot \frac{\ln(1+1/k)^{1+1/k}}{4D}\cdot\int_0^{2L} x\cdot J_0^2\left(\frac{2\pi x}{\lambda}\right)dx - \frac{1}{2L} \\ & \cdot\left\{\frac{4L^2}{2} + \frac{1}{4m}\int_0^{2L} x\cdot J_0^2\left(\frac{2\pi x}{\lambda}\right)dx\right. \\ & + \frac{\ln(1+1/k)^{1+1/k}}{4D}\cdot\int_0^{2L} x^2\cdot dx + \frac{1}{4m} \\ & \left.\cdot\frac{\ln(1+1/k)^{1+1/k}}{4D}\cdot\int_0^{2L} x^2\cdot J_0^2\left(\frac{2\pi x}{\lambda}\right)dx\right\} - L \end{aligned} \tag{A.17}$$

which after some manipulations transforms to:

$$\begin{aligned} I(L) = {} & \frac{\ln(1+1/k)^{1+1/k}}{4D}\cdot\frac{2}{3}L^2 + \frac{1}{4m} \\ & \cdot\int_0^{2L} J_0^2\left(\frac{2\pi x}{\lambda}\right)dx + \frac{1}{4m}\cdot\frac{\ln(1+1/k)^{1+1/k}}{4D} \\ & \cdot\int_0^{2L} x\cdot J_0^2\left(\frac{2\pi x}{\lambda}\right)dx - \frac{1}{2L} \\ & \cdot\frac{1}{4m}\left\{\int_0^{2L} x\cdot J_0^2\left(\frac{2\pi x}{\lambda}\right)dx + \frac{\ln(1+1/k)^{1+1/k}}{4D}\right. \\ & \left.\cdot\int_0^{2L} x^2\cdot J_0^2\left(\frac{2\pi x}{\lambda}\right)dx\right\} \end{aligned} \tag{A.18}$$

As $2L << D$, we can also presume that

$$\begin{aligned} & \frac{\ln(1+1/k)^{1+1/k}}{4D}\int_0^{2L} x^2\cdot J_0^2\left(\frac{2\pi x}{\lambda}\right)dx \\ & << \int_0^{2L} x\cdot J_0^2\left(\frac{2\pi x}{\lambda}\right)dx \end{aligned} \tag{A.19}$$

So (A.18) can justifiably be approximated as

$$\begin{aligned} I(L) \approx {} & \frac{\ln(1+1/k)^{1+1/k}}{6D}\cdot L^2 \\ & + \frac{1}{4m}\int_0^{2L} J_0^2\left(\frac{2\pi x}{\lambda}\right)dx + \frac{1}{4m} \\ & \cdot\left[\frac{\ln(1+1/k)^{1+1/k}}{4D} - \frac{1}{2L}\right] \\ & \cdot\int_0^{2L} x\cdot J_0^2\left(\frac{2\pi x}{\lambda}\right)dx. \end{aligned} \tag{A.20}$$

Now, once again, recalling that $2L << D$, as well as $\ln(1 + 1/k) < 1$, (A.20) simplifies to

$$\begin{aligned} I(L) \approx {} & \frac{\ln(1+1/k)^{1+1/k}}{6D}\cdot L^2 \\ & + \frac{1}{4m}\int_0^{2L} J_0^2\left(\frac{2\pi x}{\lambda}\right)dx - \frac{1}{4m}\cdot\frac{1}{2L} \\ & \cdot\int_0^{2L} x\cdot J_0^2\left(\frac{2\pi x}{\lambda}\right)dx. \end{aligned} \tag{A.21}$$

Moreover, we apply to (A.21) the following limit equation [36]:

$$\lim_{n\longrightarrow+\infty}\frac{1}{\ln x}\int_0^x J_\nu^2(t)\,dt = \frac{1}{\pi} \tag{A.22}$$

which we consider as

$$\int_0^{2L} J_0^2(t)\,dt = \frac{\ln 2L}{\pi} + \varepsilon \tag{A.23}$$

where, for wide range of $2L$ values (even beyond the relevant couple of hundreds of wavelengths), the constant value is $\varepsilon \approx 0.85$, implying

$$\begin{aligned} \int_0^{2L} J_0^2\left(\frac{2\pi x}{\lambda}\right)dx &= \frac{\lambda}{2\pi}\cdot\int_0^{2L} J_0^2\left(\frac{2\pi x}{\lambda}\right)\cdot d\left(\frac{2\pi x}{\lambda}\right) \\ &= \frac{\lambda}{2\pi}\cdot\int_0^{4\pi L/\lambda} J_0^2(t)\cdot dt \\ &= \frac{\lambda}{2\pi}\cdot\left[\frac{\ln((2\pi\cdot 2L)/\lambda)}{\pi} + \varepsilon\right] \\ &\approx \frac{\lambda}{2\pi} \\ &\quad\cdot\left[\frac{\ln((2\pi\cdot 2L)/\lambda)}{\pi} + 0.85\right] \end{aligned} \tag{A.24}$$

Furthermore, following the following integral solution:

$$\int_0^{2L} x\cdot J_0^2(x)\,dx = \frac{x^2}{2}\left[J_0^2(x) + J_1^2(x)\right] \tag{A.25}$$

we can write

$$\begin{aligned} & \int_0^{2L}\frac{\lambda}{2\pi}\cdot\left(\frac{2\pi x}{\lambda}\right)\cdot J_0^2\left(\frac{2\pi x}{\lambda}\right)\cdot\frac{\lambda}{2\pi}\cdot d\left(\frac{2\pi x}{\lambda}\right) \\ & = \left(\frac{\lambda}{2\pi}\right)^2\cdot\int_0^{(2\pi\cdot 2L)/\lambda} y\cdot J_0^2(y)\,dy \\ & = \left(\frac{\lambda}{2\pi}\right)^2\cdot\frac{y^2}{2}\left[J_0^2(y) + J_1^2(y)\right]\Big|_0^{4\pi L/\lambda} \\ & = \left(\frac{\lambda}{2\pi}\right)^2\cdot\frac{(4\pi L/\lambda)^2}{2}\left[J_0^2\left(\frac{4\pi L}{\lambda}\right) + J_1^2\left(\frac{4\pi L}{\lambda}\right)\right] \\ & = 2L^2\left[J_0^2\left(\frac{4\pi L}{\lambda}\right) + J_1^2\left(\frac{4\pi L}{\lambda}\right)\right] \end{aligned} \tag{A.26}$$

and so solve the remaining integral in (A.21) as follows:

$$\int_0^{2L} x \cdot J_0^2\left(\frac{2\pi x}{\lambda}\right) dx = 2L^2\left[J_0^2\left(\frac{2\pi \cdot 2L}{\lambda}\right) + J_1^2\left(\frac{2\pi \cdot 2L}{\lambda}\right)\right]. \tag{A.27}$$

Now, substituting (A.24) and (A.27) into (A.21), the latter becomes

$$I(L) \approx \frac{\ln(1+1/k)^{1+1/k}}{6D} \cdot L^2 - \frac{1}{4m} \cdot \left[J_0^2\left(\frac{2\pi \cdot 2L}{\lambda}\right) + J_1^2\left(\frac{2\pi \cdot 2L}{\lambda}\right)\right] \cdot L + \frac{\lambda}{8\pi \cdot m} \cdot \left[\frac{\ln((2\pi \cdot 2L)/\lambda)}{\pi} + 0.85\right]. \tag{A.28}$$

So, to complete the right side of (A.5), from (A.28) it follows:

$$\frac{I(L)}{2L} \approx \frac{\ln(1+1/k)^{1+1/k}}{24D} \cdot 2L - \frac{1}{8m} \cdot \left[J_0^2\left(\frac{2\pi \cdot 2L}{\lambda}\right) + J_1^2\left(\frac{2\pi \cdot 2L}{\lambda}\right)\right] + \frac{\lambda}{8\pi \cdot m} \cdot \left[\frac{\ln((2\pi \cdot 2L)/\lambda)}{\pi} + 0.85\right] \cdot \frac{1}{2L} \tag{A.29}$$

Let us now recall the following approximation for the Bessel functions of large arguments [37]:

$$J_n(x) \approx \sqrt{\frac{2}{\pi x}} \cdot \cos\left(x - \frac{n\pi}{2} - \frac{\pi}{4}\right) \tag{A.30}$$

which we apply as follows:

$$\begin{aligned} J_0\left(\frac{2\pi \cdot 2L}{\lambda}\right) &= \sqrt{\frac{\lambda}{\pi^2 \cdot 2L}} \cdot \cos\left(\frac{2\pi \cdot 2L}{\lambda} - \frac{\pi}{4}\right) \Longrightarrow \\ J_0^2\left(\frac{2\pi \cdot 2L}{\lambda}\right) &= \frac{\lambda}{\pi^2 \cdot 2L} \cdot \frac{1 - \sin(2 \cdot ((2\pi \cdot 2L)/\lambda))}{2} \\ J_1\left(\frac{2\pi \cdot 2L}{\lambda}\right) &= -\sqrt{\frac{\lambda}{\pi^2 \cdot 2L}} \cdot \cos\left(\frac{2\pi \cdot 2L}{\lambda} + \frac{\pi}{4}\right) \Longrightarrow \\ J_1^2\left(\frac{2\pi \cdot 2L}{\lambda}\right) &= \frac{\lambda}{\pi^2 \cdot 2L} \cdot \frac{1 + \sin(2 \cdot ((2\pi \cdot 2L)/\lambda))}{2} \end{aligned} \tag{A.31}$$

By substituting (A.31) in (A.29), we obtain

$$\frac{I(L)}{2L} = \frac{\ln(1+1/k)^{1+1/k}}{24D} \cdot 2L + \frac{\lambda}{8\pi^2 \cdot m} \cdot \left[\ln\left(\frac{2\pi \cdot 2L}{\lambda}\right) + 1.67\right] \cdot \frac{1}{2L}. \tag{A.32}$$

Furthermore, to calculate the left side of (A.5), i.e., $dI(l)/d2L$, we proceed by multiplying (A.32) with $2L$:

$$I(L) \approx \frac{\ln(1+1/k)^{1+1/k}}{24D} \cdot (2L)^2 + \frac{\lambda}{8\pi^2 \cdot m} \cdot \left[\ln\left(\frac{2\pi \cdot 2L}{\lambda}\right) + 1.67\right] \tag{A.33}$$

and then deriving

$$\frac{dI(L)}{d2L} = \frac{\ln(1+1/k)^{1+1/k}}{12D} \cdot 2L + \frac{\lambda}{8\pi^2 \cdot m} \cdot \frac{1}{2L}. \tag{A.34}$$

Now, following (A.5), we equalize (A.32) and (A.34):

$$\frac{\ln(1+1/k)^{1+1/k}}{24D} \cdot 2L + \frac{\lambda}{8\pi^2 \cdot m} \cdot \left[\ln\left(\frac{2\pi \cdot 2L}{\lambda}\right) + 1.67\right] \cdot \frac{1}{2L} = \frac{\ln(1+1/k)^{1+1/k}}{12D} \cdot 2L + \frac{\lambda}{8\pi^2 \cdot m} \cdot \frac{1}{2L} \tag{A.35}$$

to obtain

$$\frac{\ln(1+1/k)^{1+1/k}}{3D} \cdot (2L)^2 - \frac{\lambda}{\pi^2 \cdot m} \cdot \left[\ln\left(\frac{2\pi \cdot 2L}{\lambda}\right) + 0.67\right] = 0. \tag{A.36}$$

As D and $2L$ are expressed as multiples of λ, which makes (A.36) wavelength-independent, in order to highlight this, we rewrite the final, elementary-function-based, implicit expression for the optimal averaging path length $2L = 2L_a$:

$$\frac{\ln(1+1/k)^{1+1/k}}{3 \cdot (D/\lambda)} \cdot \left(\frac{2L}{\lambda}\right)^2 - \frac{1}{\pi^2 \cdot m} \cdot \left[\ln\left(2\pi \cdot \frac{2L}{\lambda}\right) + 0.67\right] = 0. \tag{A.37}$$

Data Availability

The authors used empirical data reported in relevant literature, listed in the article's references.

Conflicts of Interest

The authors declare that they have no conflicts of interest.

Acknowledgments

The authors appreciate valuable suggestions and dedication that they received during this research from Professor I. M. Kostic, ret. from the University of Montenegro

References

[1] P. Njemcevic, "A Novel Approach in Determination of the Appropriate Spatial Averaging Signal Length," *Wireless Personal Communications*, vol. 82, no. 3, pp. 1851–1861, 2015.

[2] R. K. Sharma and J. W. Wallace, "Experimental characterization of indoor multiuser shadowing for collaborative cognitive radio," in *Proceedings of the 3rd European Conference on Antennas and Propagation (EuCAP'09)*, pp. 3844–3848, EuCAP, Berlin, Germany, March 2009.

[3] S. Loredo, R. P. Torres, L. Valle, M. Domingo, and J. R. Pérez, "Measurements and predictions of the local mean power and small-scale fading statistics in indoor wireless environments," *Microwave and Optical Technology Letters*, vol. 24, no. 5, pp. 329–331, 2000.

[4] W. C. Y. Lee and Y. S. Yeh, "On the Estimation of the Second-Order Statistics of Log Normal Fading in Mobile Radio Environment," *IEEE Transactions on Communications*, vol. 22, no. 6, pp. 869–873, 1974.

[5] W. C. Y. Lee, "Estimate of local average power of a mobile radio signal," *IEEE Transactions on Vehicular Technology*, vol. 34, no. 1, pp. 22–27, 1985.

[6] R. A. Valenzuela, "Estimating Local Mean Signal Strength of Indoor Multipath Propagation," *IEEE Transactions on Vehicular Technology*, vol. 46, no. 1, pp. 203–212, 1997.

[7] J. M. Matias, D. de la Vega, S. Lopez, I. Pena, I. Fernandez, and P. Angueira, "Location correction factor for coverage planning tools for DRM (Digital Radio Mondiale) in the 26 MHz band," in *Proceedings of the 2008 IEEE International Symposium on Broadband Multimedia Systems and Broadcasting (BMSB)*, pp. 1–7, Las Vegas, NV, USA, March 2008.

[8] M. D. Austin and G. L. Stuber, "Velocity adaptive handoff algorithms for microcellular systems," *IEEE Transactions on Vehicular Technology*, vol. 43, no. 3, pp. 549–561, 1994.

[9] C. Tepedelenlioglu, A. Abdi, G. B. Giannakis, and M. Kaveh, "Estimation of Doppler Spread and Signal Strength in Mobile Communications with Applications to Handoff and Adaptive Transmission," in *Wireless Communications and Mobile Computing*, vol. 1, pp. 221–242, John Wiley & Sons, Ltd, Wireless Communications and Mobile Computing, March 2001.

[10] P. Njemcevic, "Local Average Signal Estimation in Nakagami-m Channels," in *Proceeding of the IEEE 6th International Symposium on Communications, Control, and Signal Processing*, Athena, Greece, 2014.

[11] P. Njemcevic and V. Lipovac, "Estimation of radio signal spatial local mean," in *Proceedings of the 24th International Conference on Software, Telecommunications and Computer Networks, SoftCOM 2016*, September 2016.

[12] D. de la Vega, S. Lopez, J. Matias et al., "Generalization of the Lee Method for the Analysis of the Signal Variability," *IEEE Transactions on Vehicular Technology*, vol. 58, no. 2, pp. 506–516, 2007.

[13] I. M. Kostic, "Analytical approach to performance analysis for channel subject to shadowing and fading," *IEE Proceedings - Communications*, vol. 6, pp. 821–827, 152.

[14] P. M. Shankar, *Fading and shadowing in wireless systems*, Springer, New York, NY, USA, 2012.

[15] A. Abdi and M. Kaveh, "On the utility of gamma PDF in modeling shadow fading (slow fading)," in *Proceedings of the IEEE VTS 50th Vehicular Technology Conference, VTC 1999-Fall*, pp. 2308–2312, September 1999.

[16] A. Sheikh, M. Handforth, and M. Abdi, "Indoor mobile radio channel at 946 MHz: measurements and modeling," in *Proceedings of the 43rd IEEE Vehicular Technology Conference*, pp. 73–76, Secaucus, NJ, USA, May 1993.

[17] A. F. Abouraddy and S. M. Elnoubi, "Statistical modeling of the indoor radio channel at 10 GHz through propagation measurements Part I: Narrow-band measurements and modeling," *IEEE Transactions on Vehicular Technology*, vol. 49, no. 5, pp. 1491–1507, 2000.

[18] H. Hashemi, M. McGuire, T. Vlasschaert, and D. Tholl, "Measurements and Modeling of Temporal Variations of the Indoor Radio Propagation Channel," *IEEE Transactions on Vehicular Technology*, vol. 43, no. 3, pp. 733–737, 1994.

[19] A. Abdi and M. Kaveh, "A comparative study of two shadow fading models in ultrawideband and other wireless systems," *IEEE Transactions on Wireless Communications*, vol. 10, no. 5, pp. 1428–1434, 2011.

[20] A. P. Prudnikov, Y. A. Brychkov, and O. I. Marichev, *Integrals and Series - Special Functions*, Nauka, Moscow, Russia, 1983.

[21] P. S. Bithas, N. C. Sagias, and P. T. Mathiopoulos, "The bivariate generalized-K (KG) distribution and its application to diversity receivers," *IEEE Transactions on Communications*, vol. 57, no. 9, pp. 2655–2662, 2009.

[22] M. Nakagami, "The m-distribution - a general formula of intensity distribution of rapid fading," in *Statistical Methods in Radio Wave Propagation*, pp. 3–36, Oxford, UK, 1960.

[23] M. Gudmundson, "Correlation model for shadow fading in mobile radio systems," *IEEE Electronics Letters*, vol. 27, no. 23, pp. 2145-2146, 1991.

[24] A. Algans, K. I. Pedersen, and P. E. Mogensen, "Experimental analysis of the joint statistical properties of azimuth spread, delay spread, and shadow fading," *IEEE Journal on Selected Areas in Communications*, vol. 20, no. 3, pp. 523–531, 2002.

[25] Z. Wang, E. K. Tameh, and A. Nix, "Simulating Correlated Shadowing in Mobile Multihop Ralay/Ad-hoc Networks," *IEEE 802.16 Broadband Wireless Access Working Group*, July 2006.

[26] A. A. Glazunov, Y. Wang, and P. Zetterberg, "Decorrelation distance characterization of long term fading of CW MIMO channels in Urban multicell environment," in *Proceedings of the 2005 18th International Conference on Applied Electromagnetics and Communications, ICECom 2005*, Dubrovnik, Croatia, October 2005.

[27] E. Perahia, D. Cox, and S. Ho, "Shadow fading cross correlation between basestations," in *Proceedings of the IEEE VTS 53rd Vehicular Technology Conference. Proceedings*, pp. 313–317, Rhodes, Greece.

[28] T. Rautiainen, K. Kalliola, and J. Juntunen, "Wideband radio propagation characteristics at 5.3 GHz in suburban environments," in *Proceedings of the 2005 IEEE 16th International Symposium on Personal, Indoor and Mobile Radio Communications, PIMRC 2005*, pp. 868–872, September 2005.

[29] D. Laselva, . Xiongwen Zhao, J. Meinila et al., "Empirical Models and Parameters for Rural and Indoor Wideband Radio Channels At 2.45 and 5.25 GHZ," in *Proceedings of the 2005 IEEE 16th International Symposium on Personal, Indoor and Mobile Radio Communications*, pp. 654–658, IEEE, Berlin, Germany.

[30] J. Liberti and T. Rappaport, "Statistics of shadowing in indoor radio channels at 900 and 1900 MHz," in *Proceedings of the IEEE Military Communications Conference (MILCOM '92)*, pp. 1066–1070, San Diego, Calif, USA.

[31] F. Van der Wijk, A. Kegel, and R. Prasad, "Assessment of a pico-cellular system using propagation measurements at 1.9 GHz for indoor wireless communications," *IEEE Transactions on Vehicular Technology*, vol. 44, no. 1, pp. 155–162, 1995.

[32] S. Baek, J. Hwang, S. Hur, and B. Kim, "A study on correlation properties of shadow fading of millimeter wave frequency

spectrum"," in *Proceedings of the 13th IEEE Annual Consumer Communications Networking Conference (CCNC*, Las Vegas, USA, January 2016.

[33] S. Sun, T. S. Rappaport, S. Rangan et al., "Propagation Path Loss Models for 5G Urban Micro- and Macro-Cellular Scenarios," in *Proceedings of the 83rd Vehicular Technology Conference (VTC Spring)*, pp. 1–6, Nanjing, China, May 2016.

[34] T. S. Rappaport, Y. Qiao, J. I. Tamir, J. N. Murdock, and E. Ben-Dor, "Cellular broadband millimeter wave propagation and angle of arrival for adaptive beam steering systems (invited paper)," in *Proceedings of the 2012 6th IEEE Radio and Wireless Week, RWW 2012 - 2012 IEEE Radio and Wireless Symposium, RWS 2012*, pp. 151–154, usa, January 2012.

[35] Wolfram math, http://functions.wolfram.com/Hypergeometric-Functions/Hypergeometric2F1/02/01/.

[36] Werner Rosenheinrich, *Tables of some indefinite integrals of Bessel functions*, U Ernst - Abbe - Hochschule Jena, University of Applied Sciences, Germany, 2003.

[37] I. H. Sneddon, *The Use of Integral Transforms*, McGraw-Hill Book Company, New York, NY, USA, 1972.